The structure and electronic density distribution in the liquid alkali metals

1993 J. Phys.: Condens. Matter 5 9261

(http://iopscience.iop.org/0953-8984/5/50/008)

J. Phys.: Condens. Matter 5 (1993) 9261–9276. Printed in the UK

The structure and electronic density distribution in the liquid alkali metals

L E González†, D J González† and K Hoshino‡

† Departamento de Física Teórica, Facultad de Ciencias, Universidad de Valladolid, 47011 Valladolid, Spain

‡ Faculty of Integrated Arts and Sciences, Hiroshima University, Hiroshima 730, Japan

Received 13 August 1993

Abstract. We present *ab initio* calculations for the electronic density distribution, and electron–ion and ion–ion correlation functions for the liquid alkali metals at conditions near the melting point. Our calculations are based on the use of the neutral pseudoatom method to derive the interionic pair potential and on the variational modified hypernetted chain integral equation theory of liquids. The resulting theory is free of adjustable parameters, using the atomic numbers as the only input data. The interionic pair potentials obtained follow the expected trends, whereas the theoretical structural functions show a good agreement with experiment.

1. Introduction

This paper presents the calculation of the ionic and electronic correlations in the liquid alkali metals at thermodynamic conditions near their triple point. Given their nature as simple s–p bonded metals they have always attracted a lot of attention, not only for their intrinsic interest but also as an important step towards the understanding of the structural features of simple liquids.

In its standard formulation, the theory of simple liquid metals comprises the following two steps: (i) the construction of a pseudopotential from which, by applying linear response theory, an effective interionic pair potential is derived; and (ii) the calculation of the liquid structure from this pair interaction, by using a liquid state theory. The use of linear response theory, in the first step, is based on the assumption that the electron–ion interaction is weak, although this is not always so. Even for sodium, some authors (Dagens 1975, Ishitobi and Chihara 1992) have suggested that the non-linear effects in the electronic screening are important in the calculation of the effective interionic pair potential and, somehow, should be taken into account in the construction of the pseudopotential.

In this work we present an approach based on effective interionic pair potentials derived from the neutral pseudoatom (NPA) method. In fact, the philosophy behind the NPA is similar to that of the pseudopotential theory and so is its domain of applicability. In conjunction with the density functional theory (DFT) it is entirely *ab initio* and it has the advantage of handling true rather than pseudo densities. Moreover, this method allows to construct an effective local pseudopotential that, within the linear response theory, generates the non-linear screening electronic charge determined by the DFT, yielding effective interionic pair potentials that are free of adjustable parameters and using the atomic numbers as the only input data. This is discussed in section 2.1.

The evaluation of the liquid structure has been carried out by resorting to the variational modified hypernetted chain (VMHNC) approximation (Rosenfeld 1986). This is an integral

0953-8984/93/509261+16$07.50

equation theory of liquids which ensures thermodynamic consistency between the energy and virial routes to the equation of state; moreover, the variational procedure in the VMHNC ensures a reasonably good thermodynamic consistency between the virial and compressibility routes, without enforcing it, which has some advantages in the case of liquid metals for reasons we have discussed in detail elsewhere (González *et al* 1991, 1992). We have also proved the theory's reliability by comparing its predictions with the results of computer simulations, both for pure (González *et al* 1991) and multicomponent systems (González *et al* 1992). We briefly discuss the VMHNC in section 2.2.

In section 3 we show the results of our calculations. First, we present the effective interionic pair potentials derived from the NPA method, discuss their characteristics and compare them with other recently proposed pair potentials. Then we present our theoretical results for the liquid structure along with the available experimental data. For the particular case of sodium, we compare our obtained electron–ion correlation functions with those recently obtained by Takeda *et al* (1989) from the analysis of the difference between the ion–ion structure factors measured by neutron and x-ray scattering. Finally, we complete the paper in section 4 with a brief discussion of our results.

2. Theory

2.1. The neutral pseudoatom model (NPA)

A liquid metal can be regarded as a conduction electron gas of mean density n_e moving through an assembly of ions, with charge Z_v and mean density $\rho = n_e/Z_v$ whose configuration is random in space and time. Moreover, the ions attract the valence electrons, which pile up around them, thus screening the ionic potential and leading to an effective interaction between the ions.

In this section we briefly describe the method for obtaining the interionic pair potentials. For additional details see Perrot (1990), Perrot and March (1990) and González *et al* (1993b).

The present approach for the calculation of the interionic pair potentials involves several steps. First, the valence electronic density displaced by an ion embedded in an homogeneous electron gas is obtained by using the NPA; then an effective local pseudopotential is constructed by requiring that within linear response theory (LRT), the same displaced density is reproduced as obtained previously. Finally, from the pseudopotential, an effective interionic pair potential is obtained. Here, we briefly discuss this process.

Within the NPA model, it is assumed that the total electronic density $\rho_e(r)$ of the metal can be decomposed as a sum of localized electronic densities, $n(r)$, that follow the ions in their movement (Hartree atomic units will be used throughout the paper)

$$\rho_e(r) = \sum_i n(|r - R_i|) = \sum_i n_c(|r - R_i|) + \sum_i n_v(|r - R_i|) \tag{1}$$

where R_i denotes the ionic positions, $n_c(r)$ is the core electronic density and $n_v(r)$ is the valence electronic density. It must be stressed that equation (1), which is based on the superposition approximation, is an approximate relation, particularly with regard to $n_v(r)$. Nevertheless, this approximation is consistent with the binary character of the interionic forces and, therefore, compatible with the usual analysis of the simple metals in terms of pair interactions.

Now, $n_v(r)$ is decomposed into two contributions denoted $n'_v(r)$ and $n''_v(r)$, that is $n_v(r) = n'_v(r) + n''_v(r)$. The first contribution, namely $n'_v(r)$, arises when a metallic ion

is introduced into a jellium in which a cavity has been made, so it represents the valence electronic density displaced by an external potential $V'_{ion}(r)$ defined as

$$V'_{ion}(r) = V_{ion}(r) + [1/r * \nu(r)] \tag{2}$$

where * denotes the convolution operation, $V_{ion}(r)$ stands for the bare ionic potential and $\nu(r)$ is a cavity screening function introduced in order to make $V'_{ion}(r)$ as weak as possible. The screening function integrates to Z_v, so for large distances it will compensate the behaviour of $V_{ion}(r)$. But for small distances, $V_{ion}(r)$ diverges as $-Z_{at}/r$, where Z_{at} is the atomic number of the ion, so $V'_{ion}(r)$ will not be weak. Moreover, the contribution of the core electrons to $V'_{ion}(r)$ is influenced by the presence of the valence electrons so $V'_{ion}(r)$ and $n'_v(r)$ must be evaluated self-consistently. This is carried out by using the density functional theory (DFT), by solving the Kohn–Sham equations for all the electrons (core and valence electrons) and where the electronic exchange and correlation effects have been included by the local-density-approximation (LDA) expression of Vosko *et al* (1980).

The second contribution to the valence electronic density, namely $n''_v(r)$, comes from the electronic valence density which screens in LRT the charge distribution associated with the cavity screening function $\nu(r)$, that is

$$\tilde{n}''_v(q) = -(4\pi/q^2)\chi(q)\nu(q) \tag{3}$$

where the tilde denotes the Fourier transform and $\chi(q)$ is the density response function. In order to be consistent with the approximation made in the previous step, the electronic exchange and correlation effects in $\chi(q)$ have been included via a LDA local field. For more details about the use of the LRT and the optimum shape of the cavity, we refer the reader to Dagens (1972, 1973, 1975) and González *et al* (1993b) and we only mention that in the present calculations $\nu(r)$ has been taken as a spherical cavity with a radius given by the Wigner–Seitz radius, R_{WS}.

Now, we turn to the calculation of a local pseudo potential, $\tilde{v}_{ps}(q)$, that within LRT reproduces the nonlinear screening charge determined by the NPA method, namely $n_v(r)$. This is achieved by first pseudizing $n_v(r)$ so as to eliminate the core orthogonality oscillations, leading to a displaced valence electronic pseudo-density, $n_{ps}(r)$, from which a pseudopotential is obtained by

$$\tilde{n}_{ps}(q) = \chi(q)\tilde{v}_{ps}(q). \tag{4}$$

Finally, application of standard second-order perturbation pseudopotential theory leads to the effective interionic pair potential, $\phi(r)$, given by

$$\phi(r) = Z_v^2/r + \phi_{ind}(r) \tag{5}$$

where the Fourier transform of $\phi_{ind}(r)$ is given by

$$\tilde{\phi}_{ind}(q) = \chi(q)|\tilde{v}_{ps}(q)|^2. \tag{6}$$

This completes the specification of the NPA method as we have applied it to compute the screening valence electronic density and the interionic pair potentials of liquid alkali metals

Table 1. Thermodynamic state (ρ, T) for which the present calculations have been carried out. Here, r_c denotes the core radius of the ECM pseudopotential.

System	ρ (A^{-3})	T (K)	r_c (au)
Na	0.024 26	373	1.77
K	0.012 71	343	2.34
Rb	0.010 30	313	2.42
Cs	0.008 34	303	2.68

at conditions near the triple point. In table 1 we show the corresponding thermodynamic states for which the present study has been carried out.

The present model is based on the idea that the electronic response to the ions in the liquid metal can be written as a superposition of single ionic responses. In this way, we solve the Kohn–Sham equations for a bare nucleus, within a spherical cavity of charge Z_v, and embedded in a jellium. As the self-consistent ion together with the screening charge associated with the cavity give rise to a weak scattering potential (the Friedel sum is zero at the Fermi level), then the superposition approximation, implied by equation (1) should be a good one for the metal.

The choice of a local effective pseudopotential, as defined in equation (4) is an *ansatz* made in order to avoid introducing any parameters, while at the same time preserving the full information contained in the calculated NPA displaced valence electronic density $n_v(r)$. In this way, we obtain a pseudopotential which in linear response theory gives rise to the non-linear displaced valence electronic density obtained by the NPA method.

2.2. *Liquid state theory: the variational modified hypernetted chain approximation (VMHNC)*

The calculation of the static structural functions of the liquid system has been carried out by using the variational modified hypernetted chain approximation (VMHNC), which is briefly described below. For additional details see Rosenfeld (1986) and González *et al* (1992).

The starting point of most integral equation theories of liquids is the Ornstein–Zernike equation, which for an homogeneous, isotropic system reads as

$$h(r) = c(r) + \rho \int c(|r - r'|)h(r')\,dr' \tag{7}$$

which defines the direct correlation function (DCF), $c(r)$, in terms of the total correlation function, $h(r) = g(r) - 1$, where $g(r)$ is the pair distribution function (PDF) and ρ is the number density. This relation is supplemented by the exact closure relation

$$c(r) = h(r) - \ln\left(g(r)e^{\beta\phi(r)+B(r)}\right) \tag{8}$$

where $\phi(r)$ is the interionic pair potential, $\beta = (k_B T)^{-1}$ is the inverse of the temperature times the Boltzmann constant and $B(r)$ denotes the bridge function, for which some approximation must be made. Following the universality assumption of bridge functions (Rosenfeld and Ashcroft 1979) we have chosen those obtained within the Percus–Yevick (PY) approximation for hard spheres, $B_{PY}(r, \eta)$. These functions only depend on one parameter—the packing fraction—and the procedure to determine it has led to different, though closely interwoven, approaches. We briefly explain the VMHNC criterion to determine this parameter.

The exact expression for the configurational Helmholtz free energy, $F'/Nk_BT \equiv f = f^{MHNC} + f^{(1)}$

$$f^{MHNC} = \frac{1}{2}\int dx\, g(x)[\beta\phi(x/\rho^{1/3}) + B(x)] - \frac{1}{2}\int dx\, [\tfrac{1}{2}h^2(x) + h(x) - g(x)\ln g(x)]$$
$$- \frac{1}{2}\frac{1}{(2\pi)^3}\int dq\{\ln[1+\tilde{h}(q)] - \tilde{h}(q)\} \tag{9}$$

and

$$f^{(1)} = -\frac{1}{2}\int_0^1 d\xi \int dx\, g_\xi(x)\frac{\partial B_\xi(x)}{\partial \xi} \tag{10}$$

where $x = r\rho^{1/3}$, the tilde denotes the Fourier transform and ξ stands for the Kirkwood charging parameter, with $g_\xi(x)$ and $B_\xi(x)$ defining the pair distribution function and bridge functions, respectively, corresponding to the potential $\phi_\xi(x/\rho^{1/3}) = \xi\phi(x/\rho^{1/3})$. Now by taking $B(x) = B_{PY}(x, \eta)$, then the MHNC free energy becomes a function of β, ρ and η. In order to choose η as a function of the thermodynamic state, that is $\eta = \eta(\beta, \rho)$, we follow a criterion of the type

$$\partial f^{MHNC}/\partial\eta = d\Delta^{(0)}(\eta)/d\eta \tag{11}$$

where $\Delta^{(0)}(\eta)$ is an arbitrary function of η only, satisfying $\Delta^{(0)}(\eta = 0) = 0$. This ensures the virial/energy consistency because

$$f^E = f^V = f^{MHNC}(\beta, \rho, \eta) - \Delta^{(0)}(\eta) \equiv f^{V\,MHNC} \tag{12}$$

where f^E and f^V represent the free energy computed through the energy and virial routes, respectively. Moreover, criterion (11) can be cast in the variational form

$$\partial f^{VMHNC}(\beta, \rho, \eta)/\partial\eta = 0. \tag{13}$$

For reasons discussed elsewhere (Rosenfeld 1986, González *et al* 1992) we write

$$\Delta^{(0)}(\eta) = f_{PY}^{MHNC}(\eta) - f_{PYV}(\eta) - \delta_\phi(\eta)$$

with

$$\delta_\phi(\eta) = f_{CS}(\eta) - f_{PYV}(\eta) \tag{14}$$

where $f_{PY}^{MHNC}(\eta)$ is the value for equation (9) when the PY–HS bridge and correlation functions with packing fraction η are used, $f_{PYV}(\eta)$ denotes the HS virial Helmholtz free energy in the PY approximation and $f_{CS}(\eta)$ denotes the empirical HS Carnahan–Starling Helmholtz free energy.

2.3. Electron–ion correlation functions

The correlation between valence electrons and ions can be described by the electron–ion structure factor $S_{ei}(q)$ and its Fourier transform, the electron–ion pair distribution function (PDF), $g_{ei}(r)$, which are simply obtained as (Chihara 1987)

$$S_{ei}(q) = Z_v^{-1/2}\tilde{n}(q)S(q) \tag{15}$$

and

$$g_{ei}(r) = 1 + \frac{1}{(n_e\rho)^{1/2}}\frac{1}{(2\pi)^3}\int S_{ei}(q)\exp(iq\cdot r)\,dq \tag{16}$$

where $\tilde{n}(q)$ stands for the screening valence electronic density and $S(q)$ represents the ion–ion static structure factor.

3. Results

3.1. Screening valence electronic density and effective interionic pair potentials

The present formulation has been applied to calculate the static structure of the liquid alkaline metals Na, K, Rb and Cs at thermodynamic conditions near the triple point.

First, the electronic core states of the ion as well as its self-consistent screening valence electronic density, $n_v(r)$, have been computed according to the prescription outlined in section 2.1. In figure 1, we show the results obtained for the screening valence electronic density and its two components $n'_V(r)$ and $n''_v(r)$. Note that $n'_v(r)$ screens a total zero charge whereas $n''_v(r)$ screens the total Z_v charge, so this explains the strong difference between both components, mainly at the core region. For large r-values, $n_V(r)$ shows the typical Friedel oscillations whose behaviour is mainly determined by $n'_v(r)$. For comparison, we have also plotted in figure 1 the linear response screening valence electronic densities obtained by using the empty-core–model pseudopotential (ECM), $\tilde{v}_{ps}(q) = -4\pi Z_v \cos(qr_c)/q^2$, along with the Ichimaru–Utsumi approximation for the local field factor, where the r_c values were chosen so as to match the first peak position of the experimental static ion–ion structure factor. Comparison shows that whereas both approaches lead to rather similar results in Na, the differences increase on going down column Ia with the empty core model producing stronger Friedel oscillations and increasing the phase shifts with respect to the NPA results. We have also included in figure 1 the ns electronic density distribution of the free atom, where n represents the quantum number of the outermost atomic shell.

The calculated interionic pair potentials are shown in figure 2. The variations found within this group follow rather well the trends suggested by Hafner and Heine (1983) which were obtained within the framework of second-order perturbation theory with the ECM pseudopotential for the bare electron–ion interaction. Nevertheless, comparison between the NPA pair potentials and the ECM ones (computed from the displaced valence electronic densities shown in figure 1) shows that whereas the repulsive parts are nearly identical there are also some differences: e.g. the principal minimum in the ECM pair potentials is deeper and narrower and the Friedel oscillations are also stronger. Within the context of a local pseudopotential, the amplitude of the Friedel oscillations in the interionic pair potential is set by a single matrix element, $\langle k+q|\tilde{v}_{ps}|k\rangle$ at $q = 2q_F$ where q_F is the Fermi wavevector, whereas for a non-local one this amplitude depends on a weighted average over non-local matrix elements, with scattering geometries ranging from forward to backward scattering. In the case of the NPA pair potentials, the ultimate reason for the shape of the Friedel oscillations must be sought in the large r-behaviour of the displaced density, $n'_v(r)$, which is set by the phase shifts of the valence electronic wave functions.

The solid crystalline structures of the alkali metals are of close-packed type, specifically of a body-centred-cubic-type structure and their experimental structure factors for the liquid state, at the triple point, suggest that a close-packed arrangement is conserved. For a liquid (and a solid too) the typical nearest-neighbour distances usually lie within the region where the pair potential changes gradually from repulsive to oscillatory behaviour. In figure 2 we have also plotted the nearest-neighbour distances (D_{cp}) for close packing, which for our NPA pair potentials lie close to the first minimum.

Several interionic pair potentials have been proposed for the liquid alkali metals, either based on local or non-local pseudopotentials. Among the latter ones we mention here those obtained by Jank and Hafner (1990, 1991), which are based on an orthogonalized-plane-wave (OPW) expansion of the conduction electronic states together with the LDA for exchange and correlation effects. Also Chihara and co-workers (Chihara 1989, Ishitobi and Chihara 1992, 1993) have obtained rather accurate pair potentials for Li, Na and K, and

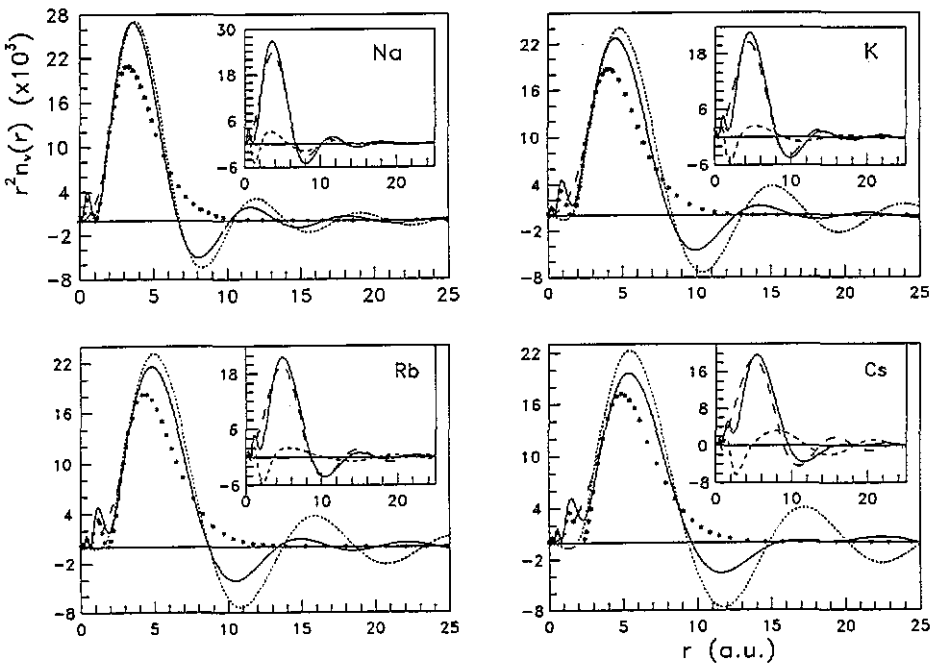

Figure 1. Displaced valence electronic densities for Na, K, Rb and Cs. The full curve shows the NPA results, the dotted curves are the results from the ECM pseudopotential, the broken curve shows the pseudized valence electronic densities, $r^2n_{ps}(r)$, and the asterisks denote the ns bound electronic density of the free atom. The inset in the figures show the total displaced valence electronic density, $r^2n_v(r)$ (full curve) and its two components, $r^2n'_v(r)$ (broken curve), and $r^2n''_v(r)$ (dotted curve).

their approach is based on an effective local pseudopotential, obtained by using the DFT in the quantal hypernetted chain method (QHNC) where the liquid metal is visualized as a nucleus–electron mixture (Chihara 1985). In fact, the present NPA method is closely related to the QHNC formulation, with the pseudopotential derived from the NPA being formally identical to the electron–ion direct correlation function of the QHNC approach.

In figure 2(a) we show, for Na, the interionic pair potential calculated by the NPA method along with other theoretical proposals. We have also included in this figure the pair potential extracted by Reatto *et al* (1986) from the measured static structure factor (Greenfield *et al* 1971). The present NPA potential exhibits a shape that reproduces qualitatively the trends appearing in the extracted potential, that is it gives the same value for the depth of the first attractive minimum, although slightly shifted to smaller r-values, and the other maxima and minima are located at practically the same positions with the extracted potential remaining negative at larger r-values. In fact, the present NPA pair potential is practically indistinguishable from the one recently obtained by Perrot and March (1990), the only difference between both approaches being the LDA expression used for the electronic exchange and correlation effects. A qualitatively similar degree of agreement with the extracted potential is also shown by the QHNC one whereas the OPW potential shows the most dissimilar features among those considered here. On the other hand, it is interesting to note that the simple ECM potential remains rather close to the NPA one.

In figures 2(b)–2(d), we show the obtained NPA potentials for K, Rb and Cs along with

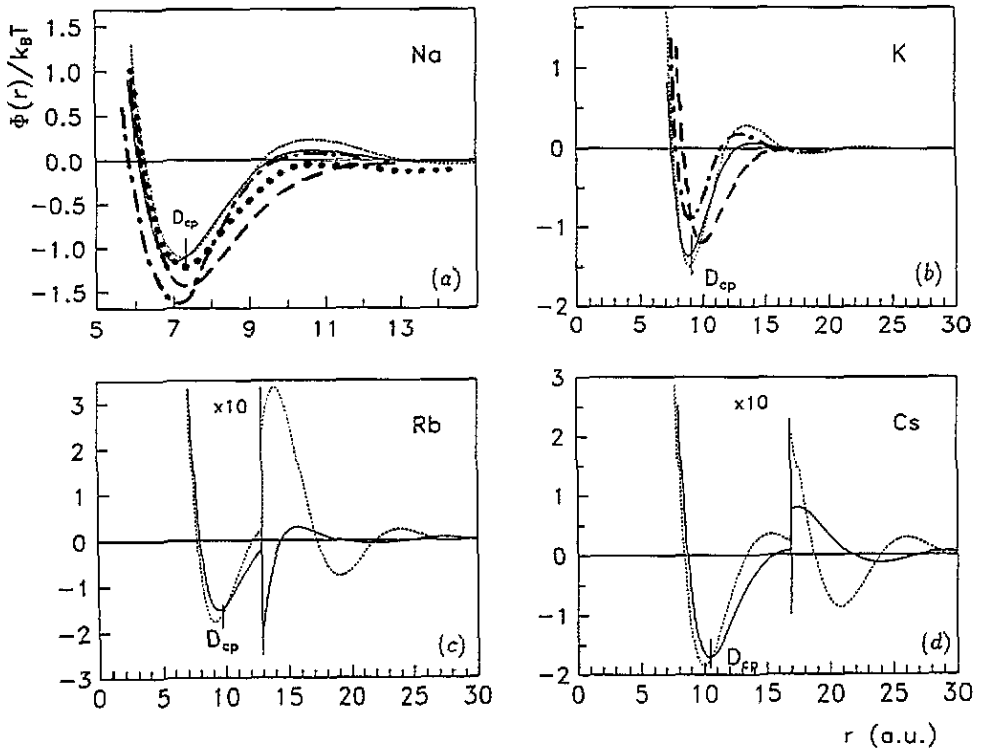

Figure 2. Interionic pair potentials for Na (*a*), K (*b*), Rb (*c*) and Cs (*d*). The full curve shows the NPA results and the dotted curves are the results used in the ECM pseudopotential. In the case of Na and K, the broken curve shows the pair potential of Ishitobi and Chihara (1992, 1993), the chain curve shows that of Jank and Hafner (1990, 1991) and the full circles show, for Na the pair potential extracted by Reatto *et al* (1986) from the experimental structure factor.

the corresponding ECM potential result; and for K we have also included the corresponding QHNC and OPW pair potentials. Comparison with the OPW potentials reveals that the differences observed for Na become enhanced on going down column Ia. In fact, although both sets of potentials predict nearly the same value for the position of the first attractive minimum, rather different values are obtained for its depth, with the NPA potentials exhibiting a deeper and broader attractive first minimum; the depth difference for Cs being larger than a factor of two. In fact, this increasing difference in the depth of the attractive first minimum is a result of the different trends shown by the NPA and OPW pair potentials. The OPW pair potentials for the alkali metals become less deep on going down column Ia, which is in opposition to the behaviour exhibited by the NPA potentials and to the trends suggested by Hafner and Heine (1983).

Moreover, it has been suggested (Perrot and Chabrier 1991) that the entropy is a very sensitive magnitude for testing the overall quality of a given interionic pair potential. We have computed the total entropy per ion (in k_B units), $s = s_{id} + s_{str} + s_{eg}$, where the three terms represent the ideal gas, the structural and the electron gas contributions, respectively, and taking for s_{eg} the free electron result (Faber 1972, González *et al* 1993a). The values obtained are as follows: 8.14 (Na), 9.49 (K), 10.72 (Rb) and 11.26 (Cs), compared with the experimental values of 7.68, 9.13, 10.26 and 11.13, respectively (Fink and Leibowitz 1985).

Finally, we end this section by mentioning another interesting feature of the present NPA interionic pair potentials. The existence of several analogies in the structural and dynamical behaviour of the liquid alkali metals has led several authors (Mountain 1977, Singh and Holz 1983, Matsuda *et al* 1991, Balucani *et al* 1992, 1993) to suggest that the interionic pair potentials should somehow, follow a law of corresponding states. By choosing as scaling magnitude the energy ϵ of the main minimum and the distance σ of the first zero of the potential, it is observed that the present rescaled NPA pair potentials do approximately follow the same curve in the case of K, Rb and Cs whereas for Na some deviations occur. In fact, similar results have also been reached by Jank and Hafner (1991) with their OPW pair potentials and also by Balucani *et al* (1992, 1993), using the model potential of Price *et al* (1970).

3.2. Liquid structural correlation functions

The calculation of the ion–ion and electron–ion structural functions for the liquid alkali metals has been carried out by combining the interionic pair potentials obtained in the previous section with the formalism outlined in sections 2.2 and 2.3.

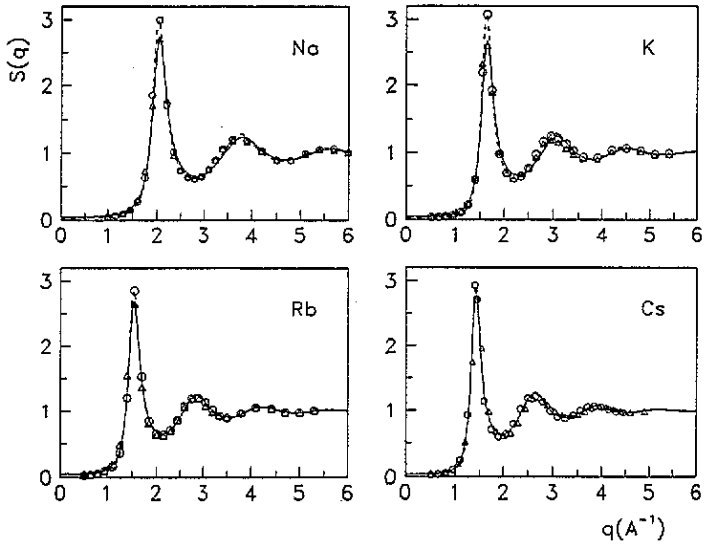

Figure 3. Ion–ion structure factors for Na, K, Rb and Cs. The full curve shows the NPA+VMHNC results, the dotted curve shows that of the ECM pseudopotential, the open circles show the x-ray data of van der Lugt and co-workers (Huijben and van der Lugt 1979, van der Lugt and Alblas 1985) for Na, K and Cs and the neutron data of Copley and Lovesey (1977) for Rb and the triangles show the x-ray data of Waseda (1980) for Na, K and Rb and the neutron data of Martin *et al* (1980) for Cs.

Figure 3 shows our calculated static ion–ion structure factors, $S(q)$, for Na, K, Rb and Cs along with the corresponding x-ray diffraction data of Waseda (1980) (for Na, K and Rb), Huijben and van der Lugt (1979) and van der Lugt and Alblas (1985) and the neutron diffraction data of Copley and Lovesey (1977) (for Rb) and Martin *et al* (1980) (for Cs). First of all, we must point out the small discrepancies shown by the different experimental data for the height of the principal peak of $S(q)$. For Na and K, the discrepancy between

both sets of experimental x-ray data is about 10%; Huijben and van der Lugt's data give an $S(q_{peak}) \simeq 3.1$ whereas those of Waseda lead to a value $\simeq 2.7$, which is in rather close agreement with our theoretical results. Similar, although smaller, discrepancies also appear in the different experimental data for Rb and Cs. Again, the x-ray data of Waseda (for Rb) and Huijben and van der Lugt (for Cs) show the bigger values when compared with the neutron data of Copley and Lovesey (for Rb) and Martin *et al* (for Cs), which closely agree with the present theoretical results.

In general, there is overall a good agreement between our theoretical $S(q)$s and the experimental data. The positions and amplitudes of the oscillations are accurately predicted, especially for Rb and Cs, whereas for Na and K there is a small shift in the position of the second peak of $S(q)$. Some discrepancies do also appear for the long-wavelength limit of the ion–ion structure factor; the present theoretical calculations give $S(q \rightarrow 0) = 0.045$ (Na), 0.048 (K), 0.054 (Rb) and 0.038 (Cs) whereas the experimental values are 0.026, 0.024, 0.022 and 0.027, respectively. Nevertheless, we find the whole agreement rather remarkable as the present theory does not resort to any adjustable parameter.

We have also included in figure 3 the $S(q)$s obtained by using the interionic pair potentials obtained from the ECM pseudopotential. The values of the core radius parameter (r_c) were determined by fitting to the position of the principal peak of $S(q)$ and, given the accuracy of the VMHNC as a liquid state theory (González *et al* 1991, 1992), we conclude that this pseudopotential can also give a good description of the ion–ion structure factor. Moreover, it also leads to some improvement in the results for $S(q \rightarrow 0)$ which are now as follows: 0.028 (Na), 0.027 (K), 0.050 (Rb) and 0.039 (Cs).

As for the other pair potentials considered in this work, we mention that by applying the Modified Hypernetted Chain (MHNC) theory of liquids to the QHNC potentials, Chihara and co-workers (Chihara 1989, Ishitobi and Chihara 1992, 1993) have also obtained, for Li, Na and K, a similar degree of agreement with the experimental structure factors. In their MHNC calculations, the packing fraction, η of the PY–HS bridge functions was chosen so as to fit the theoretical $S(q)$ to the experimental one (in Li and K) whereas in the case of Na the packing fraction was obtained by using the Lado criterion (Lado *et al* 1983). Nevertheless, their theoretical $S(q)$ do also show a similar shift in the position of the second peak, as obtained in the present calculations, although the corresponding long-wavelength-limit values do show a better agreement with the experimental results, i.e. 0.031 (Na) and 0.0206 (K).

For the OPW pair potentials, Jank and Hafner (1990, 1991) have calculated the corresponding liquid correlation functions by resorting to molecular dynamics simulations. Their results for the static structure factor show a good agreement for Na, but when going down column Ia their theoretical results show an increasing tendency to predict a higher first peak (even if compared with van der Lugt and co-workers' data) and there also appears an increasing shift in the positions of the following oscillations. In fact, this behaviour could be a reflection of the previously mentioned trends shown by the OPW pair potentials.

Now, by using equations (15) and (16), the electron–ion correlation functions are readily obtained. As equation (15) incorporates the Fourier transform of the screening valence electronic density, $\tilde{n}_v(q)$, figure 4 shows, for Na, a comparison between the theoretical NPA result and the experimental one obtained by Takeda *et al* (1989, 1990) from the difference between the static structure factors measured by x-ray and neutron diffraction experiments. Although both curves behave differently, the experimental uncertainties are so important (see figure 1 of Takeda *et al* (1990)) that the present theoretical $\tilde{n}_v(q)$ is well within those experimental uncertainties. In fact, this result is also rather similar to the QHNC result obtained by Chihara and co-workers (Chihara 1989, Ishitobi and Chihara 1992, 1993). In this figure we have not plotted the result corresponding to the screening valence electronic

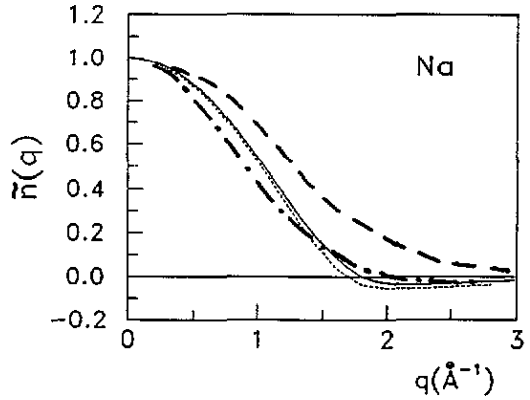

Figure 4. Screening valence electronic density, $\tilde{n}_V(q)$, of liquid Na: full curve, the NPA method; dotted curve, the ECM pseudopotential; chain curve, the 3s bound electronic density of a free atom; and broken curve, the experimental results of Takeda *et al* (1990).

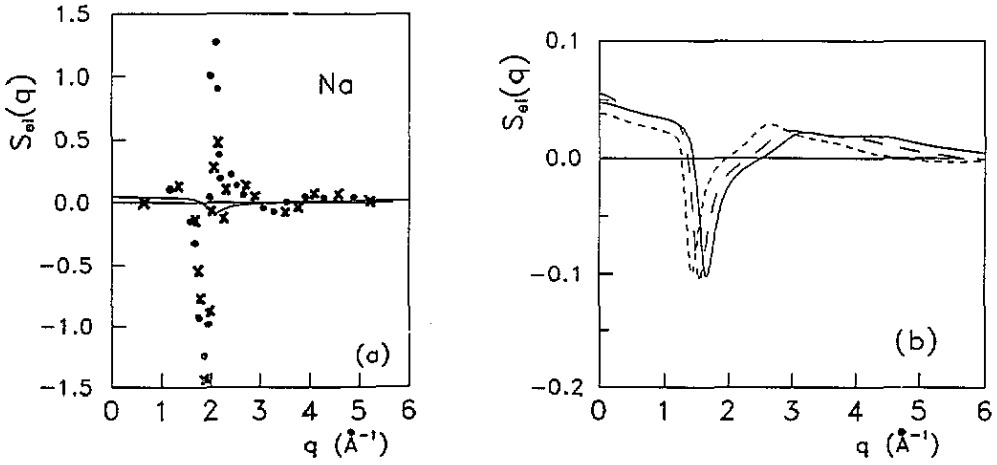

Figure 5. Electron–ion structure factors for (*a*) Na and (*b*) K, Rb and Cs. In (*a*) the full curve shows the present theoretical results whereas the full circles and the crosses represent two sets of experimental results evaluated by Takeda *et al* (1989) using either the x-ray diffraction data of Huijben and van der Lugt (1979) or those of Waseda (1980), respectively. In (*b*) the full, broken and dotted curves represent the theoretical results for K, Rb and Cs, respectively.

pseudo density, $\tilde{n}_{ps}(q)$, (see equation (4)) because, within the plotted range, it is practically indistinguishable from the real $\tilde{n}_v(q)$ and the difference between them appears in the long-range oscillations only.

Now, in figures 5(*a*) and (*b*) we show the calculated electron–ion structure factors, $S_{ei}(q)$, for the alkali metals considered in this work. The factors obtained show rather similar features, namely, they are positive in the long-wavelength region, show a dip located at the position of the main peak of the static ion–ion structure factor and the following oscillations are quickly damped. These features are in qualitative agreement with the experimental results obtained by Takeda *et al* (1989, 1990) for liquid Na although there remain important quantitative differences. Nevertheless, as pointed out by Takeda

et al (1990) the experimental data should be used with some caution because the large differences between the theoretical and experimental results are located precisely around the region of the main peak of the ion–ion static structure factor, which is quite sensitive to the experimental accuracy. This is further shown in figure 5(*a*) where we have also plotted two sets of experimental data (Takeda *et al* 1989); one was obtained by using the x-ray diffraction data of the Huijben and van der Lugt (1979) and the other was obtained by using the x-ray data of Waseda (1980).

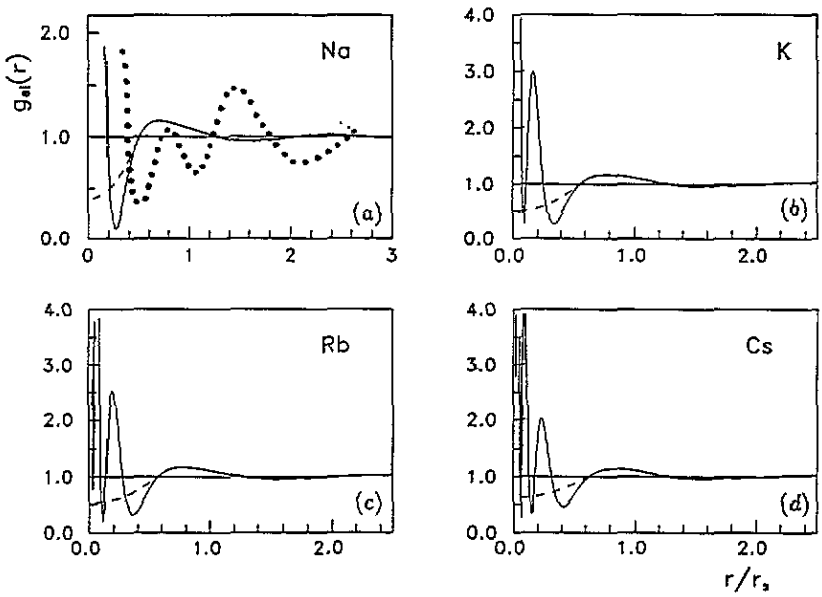

Figure 6. Electron–ion pair distribution functions for Na (*a*), K (*b*), Rb (*c*) and Cs (*d*). The full and broken curves show the NPA results obtained by using the total and the pseudized displaced valence electronic densities, respectively. The full circles represent, in Na, the experimental data of Takeda *et al* (1989). $r_s = (3/4\pi n_e)^{1/3}$ is the radius per electron.

Figures 6(*a*)–6(*d*) show the calculated electron–ion PDF, $g_{ei}(r)$, for the alkali metals considered in this work. It is observed that the $g_{ei}(r)$ have several dips (two in Na, three in K, four in Rb and five in Cs) which are correlated with those already displayed by the screening valence electronic density, $n_V(r)$, shown in figure 1. As the inner dips take rather large values, only the outer ones have been plotted in the figures. These dips are associated with the existence of bound electrons in the ionic cores, and in table 2 we list the positions of the dips as well as the average values for the distance of the orbitals of the bound electrons as obtained by the NPA method. Several comments can be made from this table:

(1) The number of dips exhibited by a given $g_{ei}(r)$ is exactly the number of non-empty atomic shells (characterized by the principal quantum number n) in the ionic core; each dip is associated with an atomic shell and it comes from the repulsion, by Pauli's principle, due to the electrons in that atomic shell. This is shown in figure 6 where we have also plotted the $g_{ei}(r)$ obtained by using in equations (15) and (16) the pseudized screening valence electronic density, $\tilde{n}_{ps}(q)$. Now it is observed that by eliminating the core orthogonality

Table 2. Average values (au) for the distance of the bound electron orbital ($\langle r\rangle$, $\langle r^2\rangle$) obtained from the present NPA calculation of the electronic density displaced by an alkaline atom embedded in a cavity at the electronic densities given in table 1; r_{min} represents the positions of the dip exhibited by the electron–ion RDF, $g_{ei}(r)$.

	Na			K			Rb			Cs		
	$\langle r\rangle$	$\langle r^2\rangle$	r_{min}	$\langle r\rangle$	$\langle r^2\rangle$	r_{min}	$\langle r\rangle$	$\langle r^2\rangle$	r_{min}	$\langle r\rangle$	$\langle r^2\rangle$	r_{min}
1s	0.1439	0.0279		0.0817	0.0090		0.0413	0.0023		0.0276	0.0010	
			0.1887			0.1080			0.0538			0.0341
2s	0.7917	0.7602		*0.3914*	*0.1816*		*0.1825*	*0.0392*		*0.1188*	*0.0166*	
2p	0.8091	0.8580		0.3520	0.1537		0.1570	0.0301		0.1010	0.0124	
			1.0772			0.4684			0.2064			0.1301
3s				1.2774	1.8937		0.5230	0.3141		0.3137	0.1122	
3p				1.4415	2.4813		0.5243	0.3212		0.3037	0.1067	
3d							*0.5240*	0.3362		0.2741	0.0886	
						1.7064			0.6250			0.3492
4s							1.4822	2.5096		0.7252	0.5935	
4p							1.7382	3.5214		0.7526	0.6445	
4d										0.8321	0.8058	
									1.9650			0.8631
5s										1.8115	3.7037	
5p										2.1115	5.1047	
5d												2.3626

oscillations all the dips are swept away and the new electron–ion PDF is identical to the real one just outside the core region.

(2) For a given atomic shell, the position of the corresponding dip in the $g_{ei}(r)$ denoted by r_{min}, is always located within the range $[\langle r\rangle_{n,l_{max}}, \langle r\rangle_{n,l_{max}} + \sigma_{n,l_{max}}]$ where (n, l_{max}) represents the non-empty electronic orbital with the highest value for the orbital quantum number l and $\sigma_{n,l_{max}}$ stands for the standard deviation corresponding to that electronic orbital.

(3) Within a given element, the standard deviation, σ_{nl} increases with the quantum numbers (nl); the biggest values appearing for the orbitals within the outermost atomic shell. This explains why the last dip in the corresponding $g_{ei}(r)$ is always the broader one.

(4) On moving down column Ia, it is also observed that there is an overall increase in the values of the σ_{nl} associated with the outermost atomic shell. This is paralleled by the broadening effect shown by the last dip of the corresponding $g_{ei}(r)$.

(5) The contraction suffered by the inner atomic shells on going down along column Ia is also reflected in the position and value of the dips. In this way, for a given principal quantum number, the corresponding dip shifts towards smaller r-values and it takes higher values; for example, the dip associated with the principal quantum number $n = 2$, ranges from a position $r_{min}(n = 2) = 1.08$ au and value $g_{ei}(r_{min}) = 0.094$ in Na to $r_{min}(n = 2) = 0.13$ au and $g_{ei}(r_{min}) = 2.8$ in Cs.

In figure 6(*a*) we have also plotted the experimental $g_{ei}(r)$ obtained by Takeda *et al* (1989, 1990) for liquid Na. Their result shows a dip located at a distance $\simeq 1.8$ au which, according to the results shown in table 2, suggests that the strong disagreement should be ascribed to inaccuracies in the experiment. In fact, similar conclusions have been reached by Hoshino and Watabe (1992) and by Chihara and co-workers (Chihara 1989, Ishitobi and Chihara 1992).

4. Summary and conclusions

We have studied the ionic and electronic correlations in the liquid alkali metals at thermodynamic conditions near their triple point. This has been carried out within the framework of the NPA method and the VMHNC theory of liquids, resulting in a whole theory free of adjustable parameters, with the atomic numbers as the only input data.

This formulation starts from the screening charge around an ion embedded into an homogeneous electron gas, which yields an effective local pseudopotential and finally an interionic pair potential. Then, application of the VMHNC theory gives the ion–ion and electron–ion liquid correlation functions. The results obtained for the ion–ion correlation functions show excellent agreement with the corresponding experimental data, as shown in figure 3. Similar results are also obtained by using the ECM-based pair potentials, so the differences found between the ECM and NPA pair potentials have practically no consequences for the ion–ion correlation functions. In a recent study for liquid lithium (González *et al* 1993a) we have reached similar conclusions not only for the ion–ion correlation functions but also for the thermodynamic properties. Nevertheless it is possible that these differences in the interionic pair potentials will show up in the calculations of the dynamic structure and ionic transport properties.

On the other hand, the results obtained for the electronic structure do show strong discrepancies with the experimental data, as shown for Na in figures 4–6. Given the extreme difficulties involved in the accurate experimental determination of this electronic structure, we think that these discrepancies are due to inaccuracies related to the experiment and, in

fact, similar claims have also been put forward by other authors (Hoshino and Watabe 1992, Ishitobi and Chihara 1992).

Finally, we point out that the present NPA+VMHNC theoretical approach lacks self-consistency because the screening charge should be computed not for an ion embedded in an homogeneous electron gas but for an ion surrounded by other ions. So the present approach must be considered as a first step in a whole self-consistent procedure where the obtained ion–ion PDF should be introduced in the NPA method to again compute the screening charge and so forth. We are presently working on this procedure and the results will be reported in due course.

Acknowledgments

DJG gratefully acknowledges the Japanese–German Centre Berlin for the provision of a fellowship that made it possible for him to visit Hiroshima University. He also warmly acknowledges the hospitality given at the laboratory of Professors M Watabe and K Hoshino where part of this work has been carried out. LEG and DJG also thank the DGICYT of Spain, through grant PB89-0352-C02-01.

References

Balucani U, Torcini A and Vallauri R 1992 *Phys. Rev.* A **46** 2159
—— 1993 *Phys. Rev.* B **47** 3011
Chihara J 1985 *J. Phys. C: Solid State Phys.* **18** 3103
—— 1987 *J. Phys. F: Met. Phys.* **17** 295
—— 1989 *Phys. Rev.* A **40** 4507
Copley J R D and Lovesey S W 1977 *Liquid Metals 1976 (Inst. Phys. Conf. Ser. 30)* ed R Evans and D A Greenwood (Bristol: Institute of Physics) p 575
Dagens L 1972 *J. Phys. C: Solid State Phys.* **5** 2333
—— 1973 *J. Physique* **34** 879
—— 1975 *J. Physique* **36** 521
Faber T E 1972 *Introduction to the Theory of Liquid Metals* (Cambridge: Cambridge University Press)
Fink J K and Leibowitz L 1985 *Handbook of Thermodynamic and Transport Properties of Alkali Metals* ed R W Ohse (Oxford: Blackwell Scientific) ch 6.3.2
González L E 1992 *PhD Thesis* Universidad de Valladolid
González L E, González D J and Silbert M 1991 *Physica* B **168** 39
—— 1992 *Phys. Rev.* A **45** 3803
González L E, González D J, Silbert M and Alonso J A 1993a *J. Phys.: Condens. Matter* **5** 4283
González L E, Meyer A, Iñiguez M P, González D J and Silbert M 1993b *Phys. Rev.* E **47** 4120
Greenfield A J, Wellendorf J and Wiser N 1971 *Phys. Rev.* A **4** 1607
Hafner J and Heine W 1983 *J. Phys. F: Met. Phys.* **13** 2479
Hoshino K and Watabe M 1992 *J. Phys. Soc. Japan* **61** 1663
Huijben M J and van der Lugt W 1979 *Acta Crystallogr.* A **35** 431
Ishitobi M and Chihara J 1992 *J. Phys.: Condens. Matter* **4** 3679
—— 1993 *J. Phys.: Condens. Matter* **5** 4315
Jank W and Hafner J 1990 *J. Phys.: Condens. Matter* **2** 5065
—— 1991 *J. Phys.: Condens. Matter* **3** 6947
Lado F, Foiles S M and Ashcroft N W 1983 *Phys. Rev.* A **28** 2374
Martin W, Freyland W, Lamparter P and Steeb S 1980 *Phys. Chem. Liq.* **10** 49
Matsuda N, Mori H, Hoshino K and Watabe M 1991 *J. Phys.: Condens. Matter* **3** 827
Mountain R D 1977 *Liquid Metals 1976 (Inst. Phys. Conf. Ser. 30)* ed R Evans and D A Greenwood (Bristol: Institute of Physics)
Perrot F 1990 *Phys. Rev.* A **42** 4871
Perrot F and Chabrier G 1991 *Phys. Rev.* A **43** 2879

Perrot F and March N 1990 *Phys. Rev.* A **41** 4521
Price D L, Singwi K S and Tosi M P 1970 *Phys. Rev.* B **2** 2983
Reatto L, Levesque D and Weis J J 1986 *Phys. Rev.* A **33** 3451
Rosenfeld Y 1986 *J. Stat. Phys.* **42** 437
Rosenfeld Y and Ashcroft N W 1979 *Phys. Rev.* A **29** 1208
Singh H B and Holz A 1983 *Phys. Rev.* A **28** 1108
Takeda S, Harada S, Tamaki S and Waseda Y 1989 *J. Phys. Soc. Japan* **58** 3999
Takeda S, Tamaki S and Waseda Y 1990 *J. Phys.: Condens. Matter* **2** 6451
van der Lugt W and Alblas B P 1985 *Handbook of Thermodynamic and Transport Properties of Alkali Metals* ed R W Ohse (Oxford: Blackwell Scientific) ch 5.1
Vosko S H, Wilk L and Nusair M 1980 *Can. J. Phys.* **58** 1200
Waseda Y 1980 *The Structure of Non-Crystalline Materials* (New York: McGraw-Hill)